NANO LETTERS

2004
Vol. 4, No. 2
293−297

# Atomistic Simulations of Double-Walled Carbon Nanotubes (DWCNTs) as Rotational Bearings

**Sulin Zhang, Wing Kim Liu, and Rodney S. Ruoff***

*Department of Mechanical Engineering, Northwestern University, 2145 Sheridan Road, Evanston, Illinois 60208*

*Received November 14, 2003; Revised Manuscript Received December 8, 2003*

**ABSTRACT**

**Atomistic simulations of double-walled carbon nanotubes (DWCNTs) as rotational bearings were performed. Molecular mechanics (MM) calculations show that the interlayer energy surface of the bearings is nearly flat. Thermal effects on the bearings were studied with molecular dynamics (MD) simulations at finite temperature. These simulations show that the interlayer corrugation against rotation, and hence the interlayer friction coefficient, is extremely small, suggesting the possible application of DWCNTs as wearless bearings. Extreme operational conditions of the bearings for which the bearings disintegrate are also reported.**

The reliability of molecular bearings has recently attracted attention.[1,2] Previous experimental and modeling work has led to poor results, both in experiment and modeling.[3,4] One of the major limitations of such microbearings is that high friction-induced wear results in rapid disintegration. Suggestions have been made that wear can be avoided by the use of atomically precise bearings.[1] Defect-free DWCNTs possess such atomically precise surfaces, thus holding promise as possible wearless nanoscale bearings. An example of another nanobearing system is that of $C_{60}$ inside different single-walled carbon nanotubes, which has been modeled with MD[5] using a new interatomic potential[6] for the weak (interlayer) interactions. A comprehensive review of CNT mechanics has recently been published.[7]

The relative motion of two contacting graphitic layers has been recently studied. Favo et al.[8] observed a slip-to-roll transition when moving a multiwalled carbon nanotube (MWCNT) on a graphite surface using an atomic force microscope tip. This slip-to-roll transition was modeled by atomistic simulations.[9,10] These studies revealed the influence of the degree of commensurability on the tube-surface friction. In contrast to this tube-surface system, DWCNTs are composed of concentric cylindrical shells. The cylindrical shells of MWCNTs might easily slide and rotate with respect to one another, forming nearly ideal nanoscale linear and rotational bearings. Yu et al.[11] measured the sliding and pullout of nested shells of a MWCNT inside a scanning electron microscope (SEM). Both a stick-slip motion and a smooth sliding between nested shells were observed for two separate MWCNTs. The sliding frictional force was determined to be $7.2 \times 10^{-5}$ nN per atom (for "MWCNT2" as discussed in ref 11), which agrees reasonably well with the estimates (around $1.5 \times 10^{-5}$ nN per atom) by Cumings and Zettl who demonstrated the controlled telescopic extensions of MWCNTs under a high-resolution transmission electron microscope (HR-TEM).[3] Note that atomic-scale wear or fatigue was not observed after repeated extension and retraction of the telescoping nanotubes.[3] The small sliding frictional force postulated by Cumings and Zettl,[3] measured by Yu and Ruoff,[11] and modeled by Kolmogorov and Crespi,[12] suggests that a MWCNT can be used to create a nanoscale oscillator with an operating frequency in the gigahertz regime.[13−15] However, as pointed out by Rivera et al.,[16] such DWCNT-based oscillators exhibit damped oscillatory behavior, with a frequency inversely proportional to the axial length of the tubes. These above studies showed an extremely small resistance against the interlayer sliding of DWCNTs along the tube axis. However, atomistic simulations of DWCNTs as rotational bearings have not yet been reported and are the focus of the present study.

Here, we report the use of atomistic simulations to investigate the interlayer friction opposing the rotation of an inner tube with respect to the outer tube for a DWCNT. The MM calculations show that the interlayer rotational corrugation depends on the circumferential periodicity of the DWCNTs. Dynamic effects on the interlayer resistance to rotation were studied using MD simulations under isothermal conditions. The energy dissipation to the external bath measures the frictional force for the bearing. The friction coefficients are then obtained, yielding information about the efficiency of DWCNTs as rotational bearings.

An example of a DWCNT bearing is shown in Figure 1. We refer to the inner tube as the shaft and the outer tube as

* Corresponding author. E-mail: r-ruoff@northwestern.edu.

10.1021/nl0350276 CCC: $27.50 
**Published on Web 01/20/2004**

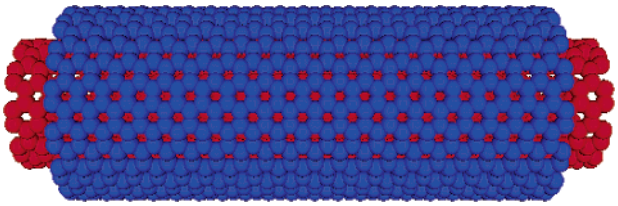

**Figure 1.** (14, 14)/(9, 9) DWCNT bearing.

the sleeve. The shaft and the sleeve have lengths of 6.0 and 5.0 nm, respectively. Two DWCNTs were considered. The shaft of each bearing was a (9, 9) CNT, and the sleeves were an armchair (14, 14) CNT and a chiral (22, 4) CNT, respectively. Note that the diameters of each sleeve tube are essentially the same: 1.89862 nm for the (14, 14) tube and 1.89867 nm for the (22, 4) tube. For each bearing, the shaft contains 900 atoms, and the sleeve contains 1176 atoms. On one end of both the shaft and the sleeve, several rings of atoms are completely fixed. On the other end, several rings of atoms are constrained in the circumferential direction, allowing the two nested nanotubes to extend and retract freely in the axial direction.

The intralayer interaction is described by a Brenner potential.[17] This potential realistically describes the bonding structure and properties of graphite and diamond and has been used to fit bond forming and breaking. As seen below, we employ this aspect to model possible failure modes of the bearings under extreme operational conditions. The interlayer interaction is represented by the registry-dependent graphitic potential recently developed by Kolmogorov and Crespi; besides the normal two-body van der Waals attraction, this registry-dependent potential accounts for the exponential atomic-core repulsion and the energy gain due to the interlayer delocalization of $\pi$ orbitals.[12] It predicts an approximately 12 meV/atom difference between AB stacking and AA stacking. Though treating the interaction region of the shaft and the sleeve as locally flat planes might lead to an overestimation of the frictional force, this potential is considered to be more realistic than the Lennard-Jones 6−12 potential.[18] To minimize the error due to the curved surfaces of the nanotubes using this potential, nanotubes with relatively large radii are chosen to constitute the bearings in our simulations.[18]

As usual, each layer of DWCNTs is indexed by two integers ($n_1$, $n_2$) that give the circumference in the lattice coordinates of the graphene sheet. The radius of the tube is $(\sqrt{3}d_0/2\pi)\sqrt{n_1^2+n_1n_2+n_2^2}$, where $d_0$ is the C−C bond length.[19] The circumferential symmetry is defined by the greatest common denominator of $n_1$ and $n_2$, GCD($n_1$, $n_2$). On the basis of the elementary number theory, the interlayer potential energy of a DWCNT bearing is periodic with a period of $\{\mathrm{GCD}(m,n)\}/mn$,[20] where the shaft and the sleeve of the molecular bearing have $m$-fold and $n$-fold symmetries, respectively. This theory suggests that for large $m$ and $n$ the shaft of the bearing has no strongly preferred circumferential position with respect to the sleeve. This implies that the interlayer potential energy surface is nearly flat for molecular bearings made of DWCNTs having a high degree of circumferential periodicity. For the DWCNT bearings considered here, the (14, 14) sleeve has 14-fold rotational symmetry, and the (22, 4) sleeve has only 2-fold rotational symmetry. Correspondingly, the period of the potential in the circumferential direction for the (14, 14)/(9, 9) bearing is $^1/_{126}$ rad, and that for the (22, 4)/(9, 9) bearing is $^1/_{18}$ rad. Thus, elementary number theory predicts that the interlayer potential energy of the (14, 14)/(9, 9) bearing should be "flatter" than that of the (22, 4)/(9, 9) bearing.

To determine the energy barrier quantitatively as a function of rotation, MM simulations were performed for the two DWCNT bearings. The shaft was rotated with respect to the sleeve by displacing the constrained atoms at the ends with a step size of $2 \times 10^{-4}$ rad. The bearing was then quasi-statically relaxed by an energy-minimization procedure employing the conjugate-gradient method. The interlayer potential energy was calculated at the minimum-energy configuration for each step. Figure 2 shows the interlayer potential per atom as a function of the circumferential position between the shaft and sleeve for the two bearings as calculated with MM. The periodicities of the interlayer potentials agree reasonably well with the theoretical prediction. We define the interlayer rotational corrugation as the

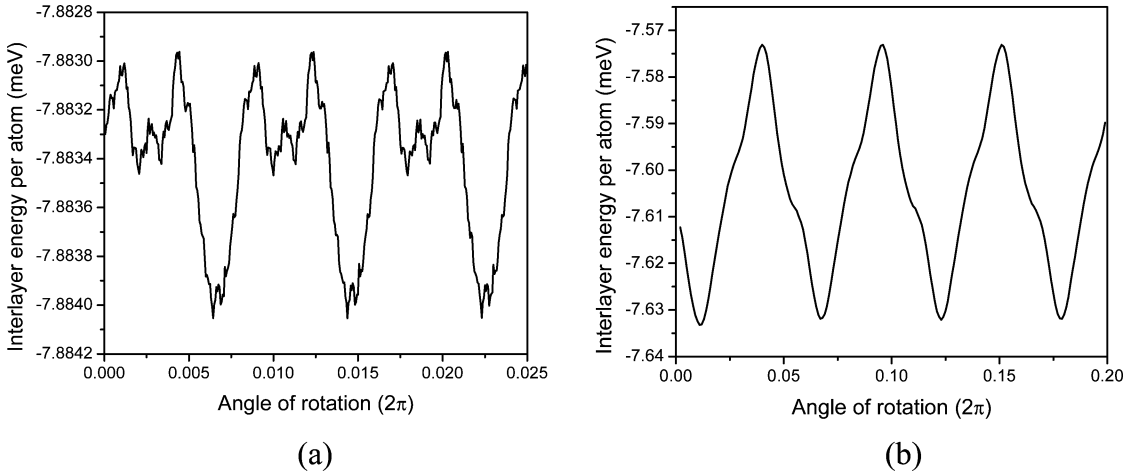


**Figure 2.** MM calculations of interlayer potentials of two DWCNT bearings. (a) (14, 14)/(9, 9) bearing. (b) (22, 4)/(9, 9) bearing.

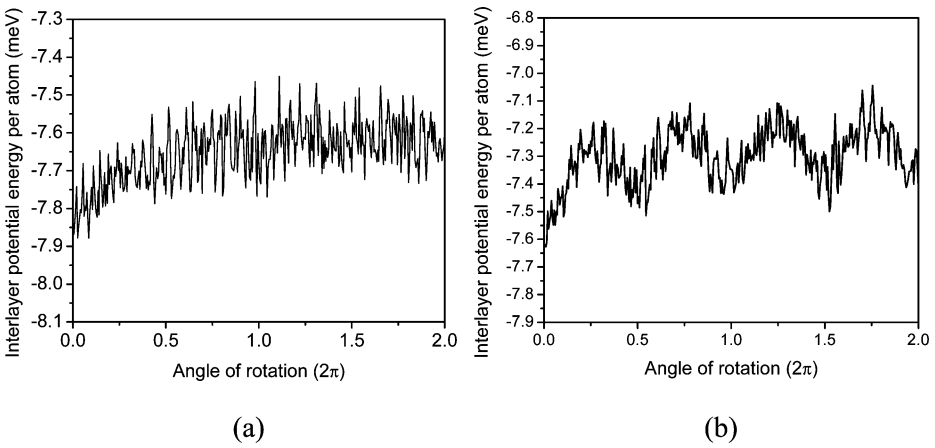


**Figure 3.** Potential energy as a function of rotation. (a) (14, 14)/(9, 9) bearing. (b) (22, 4)/(9, 9) bearing.

maximal variation in the interlayer potential energy as the shaft rotates around the sleeve, similar to the definition used by Kolmogorov and Crespi for axial sliding.[12] The higher degree of circumferential periodicity clearly leads to smaller interlayer corrugation. The rotational corrugation for the (22, 4)/(9, 9) bearing is ∼0.06 meV/atom but only ∼0.001 meV/atom for the (14, 14)/(9, 9) bearing. Both are at least 1 order of magnitude smaller than the corrugations for axial sliding for the same system size.[12] Because of the extremely high degree of circumferential periodicity of the interlayer potential energy for the (14, 14)/(9, 9) bearing, it was necessary to calculate the energy as a function of a very small rotational step size, as shown in Figure 2a.

Bearings, of course, will rotate in ways that may not be quasi-static, and the MM simulations may not fully capture the energy-dissipation mechanisms during dynamic sliding or rotation. During the dynamic process, both radial and in-plane distortions may occur. The radial distortion of the shells due to thermal vibration could hinder interlayer rotation, leading to an increase in the interlayer friction. In what follows, MD simulations were used to study dynamic effects on the interlayer friction against rotation for these two bearings. In the MD simulations, the shaft was rotated with respect to the sleeve by displacing the constrained atoms at the ends of the shaft. The rotational velocity was determined by the angular displacement applied to the constrained atoms at each time step. The equations of motion were integrated using a fifth-order predictor−corrector algorithm. The interlayer potential, the normal force, and the dissipated energy of the bearings were calculated. Extreme operating conditions that might determine the lifetime of such bearings were also investigated.

To simulate isothermal rotation, the DWCNT system was coupled to an external heat bath at room temperature (300 K) by Brendsen's method.[21] Prior to rotation, the systems are thermostated to the temperature of the external heat bath. The time constant in Brendsen's method is chosen such that the kinetic temperature of the system during rotation fluctuates within 10 K of the temperature of the external heat bath. When displacing the constrained end atoms of the shaft, elastic strain is induced between the displaced atoms and those adjacent to them. These adjacent atoms then passively rotate in order to release the accumulated strain. Previous work on nanoscale friction used the same approach as that typically used in continuum mechanics to calculate the friction coefficient (i.e., the ratio of the average frictional force to the average normal force).[22] However, ambiguities arise because the atomic frictional force calculated from MD simulations is frequently found to be negative.[22] A more realistic method for estimating the frictional force is to calculate the energy dissipation due to friction, as shown below.

When the shaft is rotated with respect to the sleeve, energy conservation requires that the external work done ($\Delta W$) by the rotational forces be equal to the changes in the potential energy ($\Delta P$) and the kinetic energy ($\Delta E$) of the bearings plus the heat ($\Delta H$) generated by friction. To hold the temperature of the system constant, the heat generated by friction was dissipated to the heat bath through Langevin atoms. The heat generated by friction can be written as

$$\Delta H = \sum_n \sum_i \mathbf{f}_i^{\text{damp}} \cdot \mathbf{v}_i \Delta t \tag{1}$$

where $i$ sums over all of the Langevin atoms in the system, $n$ sums over all of the time steps in the simulation, $\mathbf{v}_i$ is the velocity of atoms $i$, and $\mathbf{f}_i^{\text{damp}}$ is the damping force for Langevin atom $i$, expressed as

$$\mathbf{f}_i^{\text{damp}} = m_i \gamma \left( \frac{T_0}{T} - 1 \right) \mathbf{v}_i \tag{2}$$

where $T_0$ and $T$ are the reference temperature of the heat bath and the current temperature of the system, respectively, $\gamma$ is the damping constant that determines the strength of the coupling to the external bath, and $m_i$ is the mass of atom $i$. The average frictional force over $N$ rotations is thus

$$f_{\text{av}} = \frac{\Delta H}{2N\pi r} \tag{3}$$

where $r$ is taken to be the average of the radius of the shaft and the sleeve.

Figure 3 shows the potential energy as a function of ro-

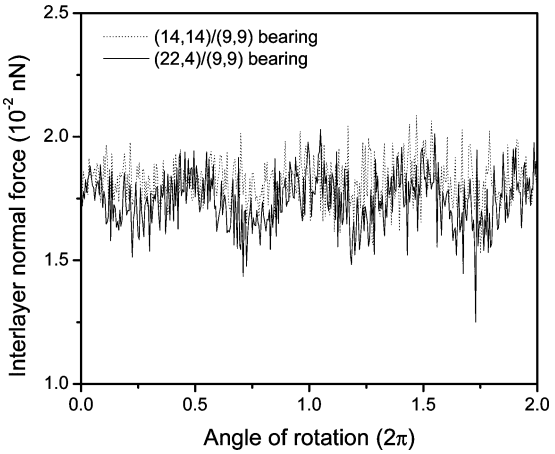


**Figure 4.** Interlayer normal forces for each DWCNT bearing.

tation for the (14, 14)/(9, 9) and (22, 4)/(9, 9) bearings. The rotation rate is 0.05 rotations per picosecond. Apparently the circumferential symmetry of the interlayer potential energy, as calculated in the MM simulations, breaks down due to dynamic effects. Different frictional responses are indicated from the interlayer potential energies for each bearing at steady state. For the (22, 4)/(9, 9) bearing, the rotational energy is roughly periodic, with a potential energy cycling through a minimum twice for each rotation. This could lead to atomic-scale locking between the sleeve and the shaft. For the (14, 14)/(9, 9) bearing, the rotational-energy corrugation is ∼0.32 meV, and for the (22, 4)/(9, 9) bearing, the rotational-energy corrugation is ∼0.45 meV. A short-time transient response appears in the initial stage of rotation for each bearing, and for this reason, the potential energy as a function of rotation was extracted from the data when the steady state was reached (∼$^3/_4$ rotation, Figure 3a and b, see also the transients present in Figure 5). Compared with the results of the MM simulations, the energy corrugation is at least an order of magnitude larger for each bearing, indicating that dynamic effects dominate interlayer friction. Figure 4 shows the interlayer normal forces for both cases. In steady-state rotation, the average normal force is 1.82 nN/atom for the (14, 14)/(9, 9) bearing and 1.75 nN/atom for the (22, 4)/(9, 9) bearing. The slightly higher average normal force for the (14, 14)/(9, 9) bearing is possibly due to the slightly smaller radius of the CNT (14, 14) compared to that of the CNT (22, 4); it could also be due to the higher rotational symmetry, which may mean that, on average, there are more "A−A" interactions versus "A−B" interactions for the (14, 14)/(9, 9) DWCNT compared to the (22, 4)/(9, 9) DWCNT.

Figure 5 shows the dissipated energy as a function of rotation time. In the initial stage of rotation, the dissipated energy exhibits large fluctuations, corresponding to the rapid exchange of energy between the bearing and the external bath. It then reaches a steady-state condition during which the dissipated energy linearly increases with time. A linear fitting of the steady-state portion shows that the energy-dissipation rate is 3.3 meV/atom per rotation for the (14, 14)/(9, 9) bearing and 3.7 meV/atom per rotation for the (22, 4)/(9, 9) bearing. The average frictional force is obtained on the basis of the calculated energy-dissipation rate using eq 3. It is found that the interlayer friction against rotation is extremely small. The average frictional force is $1.07 \times 10^{-4}$ nN per atom for the (14, 14)/(9, 9) bearing and $1.20 \times 10^{-4}$ nN per atom for the (22, 4)/(9, 9) bearing. The friction coefficients are $5.9 \times 10^{-5}$ for the (14, 14)/(9, 9) bearing and $6.9 \times 10^{-5}$ for the (22, 4)/(9, 9) bearing. Such small friction coefficients indicate that wear may not occur during operation.

The dissipation rate, and hence the friction coefficients of the bearings, are strongly dependent on the operating rate and load. To study the effect of rotational velocity, different rotational velocities were applied to the (22, 4)/(9, 9) bearing at 300 K. The rotational velocity was controlled by applying incremental angular displacements to the constrained atoms at the ends of the shaft for each time step. The energy-dissipation rate increases with increasing rotational velocity as shown in Figure 6. At 0.5 rotations per picosecond, a large distortion appeared near the ends of the shaft at the initial stage of rotation, as seen in Figure 7. The deformation of the sleeve, however, remained small. The strain energy accumulated in the shaft due to the distortion was gradually released with further rotation. At 0.75 rotations per picosecond, the rotation-induced strain near the ends of the shaft

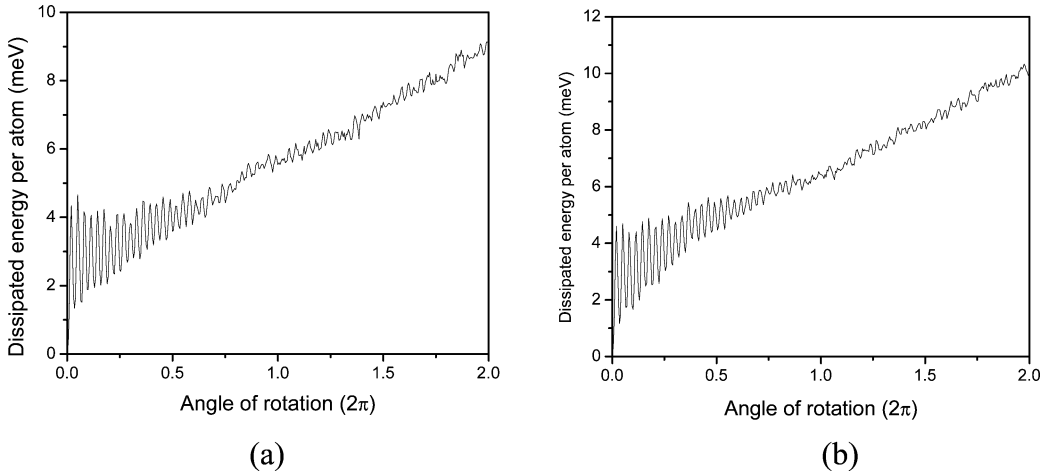


**Figure 5.** Dissipated energy. (a) (14, 14)/(9, 9) bearing. (b) (22, 4)/(9, 9) bearing.

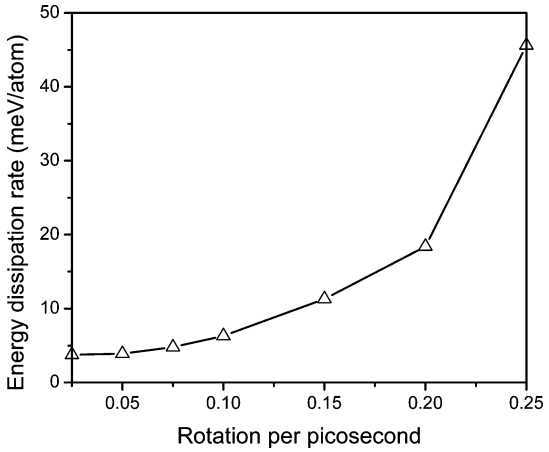


**Figure 6.** Effect of rotational rate on energy dissipation.

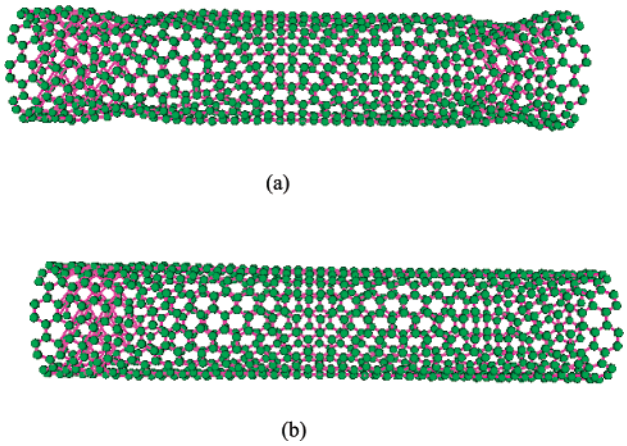


**Figure 7.** Distortions of the shaft at 0.5 rotations per picosecond. (a) Distortions near the ends of the shaft at 0.4 rotations. (b) The strain was released with continuing rotations.

could not be released prior to a large radial distortion of the sleeve. Further rotations caused the collapse of the bearing; this was the critical threshold for failure. An example of the collapsed configuration is shown in Figure 8.

In conclusion, DWCNT-based bearings were studied using MM and constant-temperature (300 K) MD simulations. The MM calculations show that the interlayer potential energy surface is nearly flat with a period of $\{\mathrm{GCD}(m, n)\}/\{mn\}$. This circumferential symmetry breaks down when the dynamic effects are included, and MD simulations show that dynamic effects dominate the friction in these DWCNT bearings. However, the resulting frictional force is still small and on the order of $10^{-4}$ nN/atom, with a friction coefficient on the order of $10^{-5}$. Our simulations (analogous to operation in vacuum) also show that the bearings work well if the rotational rate is well below 0.5 rotations per picosecond. The extremely small interlayer friction means that wear for typical rotational frequencies may not occur at all, making nanotube-based bearings a fascinating candidate for MEMS and NEMS applications.

**Acknowledgment.** R.S.R. and W.K.L. acknowledge support from the following grant: Nanorope Mechanics, NSF no. 0200797 (Oscar Dillon and Ken Chong, Program Managers). R.S.R. gratefully acknowledges a Mechanics of Nanostructures grant (award no. N000140210870) from the Office of Naval Research and a grant from the NASA University Research, Engineering and Technology Institute on Bio Inspired Materials (BIMat) (award no. NCC-1-02037). Helpful discussions with Aleksy N. Kolmogrov are acknowledged. We also thank Michael A. Peshkin and Frank T. Fisher for helpful comments.

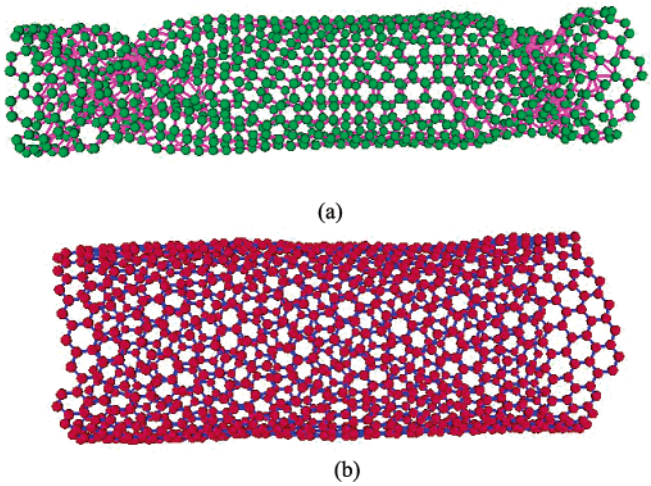


**Figure 8.** Failure of the (22, 4)/(9, 9) bearing at a critical rotational rate of 0.75 rotations per picosecond. (a) Shaft. (b) Sleeve.

## References

(1) Drexler, K. E. *Nanosystems*: *Molecular Machinery, Manufacturing and Computation*; Wiley: New York, 1992.
(2) Cumings, J.; Zettl, A. *Science* **2000**, *289*, 602.
(3) Deng, K.; Ko, W. H. *J. Micromech. Microeng.* **1992**, *2*, 14.
(4) Pelrine, R. E. Room Temperature, Open-Loop Levitation of Microdevices Using Diamagnetic Materials. In *Proc. − IEEE Micro Electro Mech. Syst.* Napa Valley, CA, 1990; p 34.
(5) Qian, D.; Liu, W. K.; Ruoff, R. S. *J. Phys. Chem. B* **2001**, *105*, 10753.
(6) Qian, D.; Liu, W. K.; Ruoff, R. S. *Compos. Sci. Technol.* **2003**, *63*, 1561.
(7) Qian, D.; Wagner, G. J.; Liu, W. K.; Yu, M.-F.; Ruoff, R. S. *Appl. Mech. Rev.* **2002**, *55*, 495.
(8) Falvo, M. R.; Tayor, R. M., II; Helser, A.; Chi, V.; Brooks, F. P., Jr.; Washburn, S.; Superfine, R. *Nature* **1999**, *397*, 236.
(9) Buldum, A.; Lu, J. P. *Phys. Rev. B* **1999**, *83*, 5050.
(10) Schall, J. D.; Brenner, D. W. *Mol. Simul.* **2000**, *25*, 73.
(11) Yu, M.-F.; Yakobson, B. I.; Ruoff, R. S. *J. Phys. Chem. B* **2000**, *104*, 8764.
(12) Kolmogorov, A. N.; Crespi, V. H. *Phys. Rev. Lett.* **2000**, *85*, 4727.
(13) Legoas, S. B.; Coluci, V. R.; Braga, S. F.; Coura, P. Z.; Dantas, S. O.; Galvão, D. S. *Phys. Rev. Lett.* **2003**, *90*, 055504.
(14) Zheng, Q.-S.; Jiang, Q. *Phys. Rev. Lett.* **2002**, *88*, 045503.
(15) Zhang, Q.-S.; Liu, J. Z.; Jiang, Q. *Phys. Rev. B* **2002**, *65*, 245406.
(16) Rivera, J. L.; McCabe, C.; Cummings, P. T. *Nano Lett.* **2003**, *3*, 1001.
(17) Brenner, D. W. *Phys. Rev. B* **1990**, *42*, 9548.
(18) Personal communications with Aleksey N. Kolmogorov, Department of Physics, The Pennsylvania State University.
(19) Dresselhaus, M. S.; Dresselhaus, G.; Eklund, P. C. *Science of Fullerenes and Carbon Nanotubes*; Academic Press: New York, 1996.
(20) Merkle, R. C. *Nanotechnology* **1993**, *4*, 86.
(21) Berendsen, H. J. C.; Postma, J. P. M.; van Gunsteren, W. F.; DiNola, A.; Haak, J. R. *J. Chem. Phys.* **1984**, *81*, 3684.
(22) Harrison, J. A.; White, C. T.; Colton, R. J.; Brenner, D. W. *Phys. Rev. B* **1992**, *46*, 9700.

NL0350276